

# First measurement of HI 21 cm emission from a GRB host galaxy indicates a post-merger system

Maryam Arabalsamani<sup>1,2\*</sup>, Sambit Roychowdhury<sup>3</sup>, Martin Zwaan<sup>1</sup>, Nissim Kanekar<sup>4</sup>, Michał J. Michałowski<sup>5</sup>

<sup>1</sup>European Southern Observatory, Karl-Schwarzschild-Strasse 2, 85748 Garching bei München, Germany

<sup>2</sup>Dark Cosmology Centre, Niels Bohr Institute, University of Copenhagen, Juliane Maries Vej 30, DK-2100 Copenhagen Ø, Denmark

<sup>3</sup>Max-Planck-Institut für Astrophysik, Karl-Schwarzschild-Strasse 1, 85748 Garching bei München, Germany

<sup>4</sup>National Centre for Radio Astrophysics, Tata Institute of Fundamental Research, Post Bag 3, Ganeshkhind, Pune 411 007, India

<sup>5</sup>Institute for Astronomy, University of Edinburgh, Royal Observatory, Blackford Hill, Edinburgh EH9 3HJ, UK

## ABSTRACT

We report the detection and mapping of atomic hydrogen in HI 21 cm emission from ESO 184-G82, the host galaxy of the gamma ray burst 980425. This is the first instance where HI in emission has been detected from a galaxy hosting a gamma ray burst. ESO 184-G82 is an isolated galaxy and contains a Wolf-Rayet region close to the location of the gamma ray burst and the associated supernova, SN 1998bw. This is one of the most luminous HI regions identified in the local Universe, with a very high inferred density of star formation. The HI 21 cm observations reveal a high HI mass for the galaxy, twice as large as the stellar mass. The spatial and velocity distribution of the HI 21 cm emission reveals a disturbed rotating gas disk, which suggests that the galaxy has undergone a recent minor merger that disrupted its rotation. We find that the Wolf-Rayet region and the gamma ray burst are both located in the highest HI column density region of the galaxy. We speculate that the merger event has resulted in shock compression of the gas, triggering extreme star formation activity, and resulting in the formation of both the Wolf-Rayet region and the gamma ray burst. The high HI column density environment of the GRB is consistent with the high HI column densities seen in absorption in the host galaxies of high redshift gamma ray bursts.

**Key words:** gamma-ray burst: general – galaxies: ISM – galaxies: star formation – galaxies: kinematics and dynamics – galaxies: interactions – radio lines: galaxies

## 1 INTRODUCTION

Long-duration gamma ray bursts (GRBs) are believed to originate in the death of short-lived massive stars and hence are expected to be located in regions with high star formation (Bloom et al. 2002; Fruchter et al. 2006). This picture is in good agreement with the high star formation rates (SFRs) typically observed in galaxies hosting GRBs. While determining the stellar mass and the SFR of GRB host galaxies at high redshifts remains challenging even with today’s 10m-class telescopes, such estimates have been possible for a fair number of GRB hosts out to  $z \sim 3$  (e.g. Castro Cerón et al. 2010). This remarkable recent progress in studies of GRB host galaxies has not been mirrored in emission studies of their neutral gas, which is the fuel for star formation. Such studies are critical in order to understand the interplay between interstellar medium (ISM) conditions and star formation that gives rise to the GRB progenitors. The neutral atomic hydrogen in several

GRB host galaxies at  $z \gtrsim 2$  has been detected in absorption, yielding estimates of the HI column density,  $N(\text{HI})$ , and gas kinematics (e.g. Fynbo et al. 2009; Prochaska et al. 2008; Arabalsamani et al. 2015). Indeed, molecular hydrogen has also been detected in absorption in three GRB hosts (Prochaska et al. 2009; Krühler et al. 2013; D’Elia et al. 2014). However, these absorption features only trace the gas along the narrow beam in the GRB sightline and carry little information on the whole galaxy. Understanding the nature of GRB host galaxies and the conditions for GRB formation critically requires emission studies in the atomic and molecular gas. Although CO emission has recently been detected in three galaxies hosting GRBs (Hatsukade et al. 2014; Stanway et al. 2015), uncertainties in the CO-to-H<sub>2</sub> conversion factor (e.g. Bolatto et al. 2013) imply large uncertainties in the inferred molecular gas mass. Unfortunately, the sensitivity of today’s radio telescopes limits HI 21 cm emission studies to relatively low redshifts,  $z \lesssim 0.2$  (e.g. Catinella & Cortese 2015). To date, the information on the HI mass, which is likely to be the dominant part of the gas content of such galaxies, does not exist for any GRB host. The HI 21 cm emission

\* E-mail: marabsal@eso.org

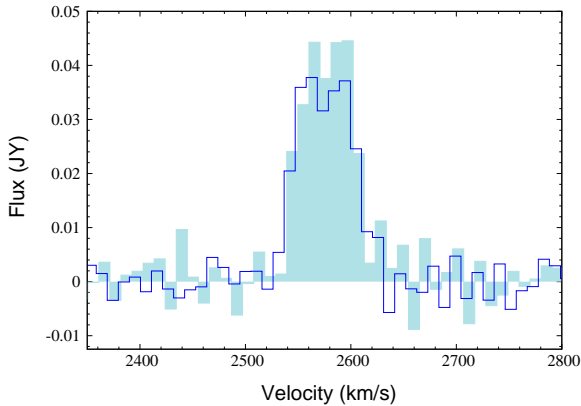


**Figure 1.** HI 21cm emission profile of the galaxy ESO 184-G82, as measured with the GMRT (shaded histogram) and the ATCA (bold line).

line would allow a direct measurement of the total HI mass, as well as detailed studies of the spatial distribution and the kinematics of the atomic gas. Combining this information on the HI content, distribution and kinematics, with information on the star formation and the stellar mass, and, finally, with information on the molecular gas, would enable us to have a comprehensive picture of galaxies hosting GRBs.

The galaxy ESO 184-G82, the host of the closest known GRB (at  $z = 0.0087$ ; Foley et al. 2006) and one of the first GRBs to be associated with a supernova (SN 1998bw, Galama et al. 1998), is one of the few GRB hosts where it is possible to carry out spatially-resolved spectroscopy and photometry. It hence offers the unique opportunity of a detailed study of the close environment of a GRB. The GRB occurred in one of the several high surface brightness star-forming regions of the galaxy (Fynbo et al. 2000). The host galaxy has a high specific star formation rate (SFR per unit stellar mass, sSFR); in particular, it contains a Wolf-Rayet (W-R) region with extremely high ongoing star formation, close to the GRB location. The cause of this high star formation has been an unsolved puzzle over the last decade. In this Letter, we present evidence for the possible cause of the extreme star formation properties of ESO 184-G82, via a study of the HI 21 cm line emission from this galaxy. This is the first time that HI has been detected in emission from a GRB host galaxy (see also Michalowski et al., in press).

## 2 OBSERVATIONS, DATA ANALYSIS AND RESULTS

We initially obtained archival Australia Telescope Compact Array (ATCA) data covering the redshifted HI 21 cm line from the GRB 980425 host galaxy (project code: C2700). These observations were carried out on 2012 April 12 in the 1.5B configuration, with a total on-source time of 8 hours, using the Compact Array Broadband Backend with a bandwidth of 3.5 MHz. The ATCA data were analysed using “classic” AIPS, following standard procedures, and yielded a detection of HI 21 cm emission from the GRB host galaxy. Since the ATCA has only six antennas, and hence relatively poor U-V coverage in a single configuration, we followed up this detection with mapping observations with the Giant Metrewave Radio Telescope (GMRT). The GMRT HI 21 cm observations of the GRB host galaxy were carried out on 2015 April 3 and 5, using a bandwidth of 4 MHz, centred at the redshifted HI 21 cm line frequency of 1410.33 MHz and sub-divided into 512 channels. The total on-source time was 2.6 hours, with observations of the standard

calibrators 3C48 and 2005-489 used to calibrate the flux density scale, the system bandpass and the system gain. The initial data editing and calibration of the GMRT data were carried out in the FLAGCAL software package (Prasad & Chengalur 2012), with the remaining analysis done in AIPS, again following standard procedures. After Hanning smoothing, re-sampling, and a detailed self-calibration process, the radio continuum was subtracted from the calibrated visibilities using the tasks UVSUB and UVLIN, and the residual visibilities mapped with different U-V tapers to produce spectral cubes at different spatial and velocity resolutions. The velocity resolution was varied in order to improve the statistical significance of the detected HI 21 cm emission in independent velocity channels. The properties of the spectral cubes that will be used here are listed in Table 1.

Fig. 1 shows the HI 21 cm emission spectra obtained from the ATCA and GMRT spectral cubes, at, respectively, spatial resolutions of  $34.5'' \times 21.4''$  and  $36'' \times 22''$  and velocity resolutions of  $10.5 \text{ km s}^{-1}$  for both datasets. Note that the spectra show the integrated flux density over the entire spatial extent of the detected HI 21 cm emission. We have checked that all of the source flux density is recovered at this resolution; further lowering the resolution does not increase the total flux density. The ATCA and GMRT spectra are seen to be in agreement; since the GMRT data have far better U-V coverage than the ATCA data, and also yield a significantly better angular resolution, all the following results and discussion will be based on the GMRT data. We obtain an integrated HI 21 cm line flux density of  $3.0 \pm 0.2 \text{ Jy km s}^{-1}$  from the GMRT spectrum of Fig. 1. Using a source distance of 37.7 Mpc (assuming a flat  $\Lambda$ -cold dark matter cosmology with  $H_0 = 69.6 \text{ km s}^{-1} \text{ Mpc}^{-1}$  and  $\Omega_m = 0.3$ ), this yields an HI mass of  $(1.00 \pm 0.08) \times 10^9 M_\odot$ . Using the coarsest resolution HI 21 cm map we measure the inclination angle of the HI disk to be between  $42^\circ$  and  $50^\circ$  for an intrinsic axial ratio varying between 0.1 and 0.5. This range in inclination is consistent with the inclination angle of the optical disk,  $i = 50^\circ$  (Christensen et al. 2008). The velocity width between half-power points is  $W_{50} = 65 \text{ km s}^{-1}$ . Correcting this for the inclination angle of  $i = 50^\circ$  yields a velocity width of  $W_{50}^i = 85 \text{ km s}^{-1}$ . The AIPS task MOMNT was used to make HI column density maps of the field, using the  $7 \text{ km s}^{-1}$  resolution data cubes, at different spatial resolutions. Fig. 2 shows three of these maps (in contours) overlaid on an Hubble Space Telescope (HST) optical image (with the MIRVIS filter, centred at  $5737.453 \text{ \AA}$ ; in greyscale). The top panel shows that the HI disk of the galaxy is more extended than the optical disk, a feature common in sub- $L_*$ , gas-rich galaxies (e.g. Begum et al. 2008). The broad peak of the HI distribution at the coarsest resolutions corresponds to the location of the optical galaxy. The intermediate-resolution ( $15'' \times 11''$ ) map, in the middle panel of Fig. 2, shows an arc of dense gas roughly coincident with the southern spiral arm of the galaxy. The W-R region mentioned above arises in one of the denser HI regions. There appears to be a lack of high-N(HI) gas at the centre of the galaxy, as well as towards the north-east of the optical disk. An apparently isolated high-N(HI) knot is visible at the extreme north-east end of the HI disk; its signature is clear in even the low resolution map. The highest resolution ( $9'' \times 5''$ ) map, shown in the bottom panel of Fig. 2, is sensitive to only the highest HI column densities. This image confirms that both the W-R region and the GRB location are coincident with the highest N(HI) regions of the galaxy. Indeed, when inspecting the N(HI) maps at higher resolution, we notice a piling up of gas on the western side of the galaxy.

To fully understand the nature of the HI distribution in the galaxy, one needs to study the velocity distribution of the gas. The

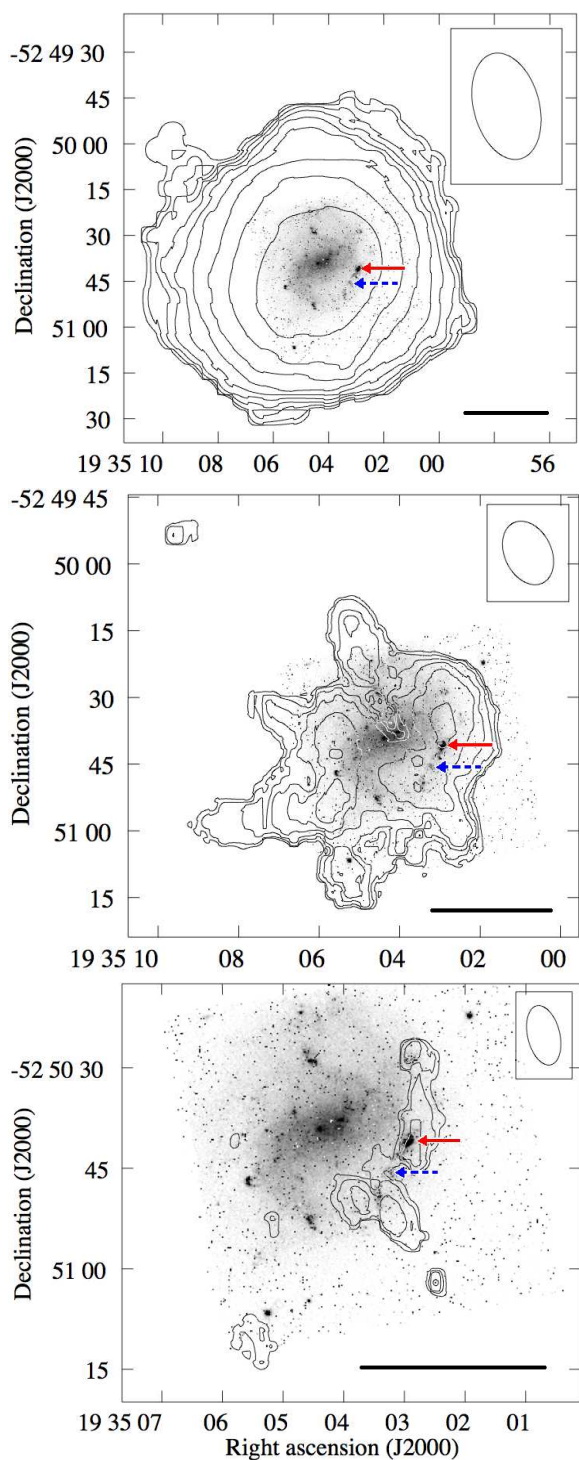


**Figure 2.** HI column density maps (in contours) overlaid on an HST image (greyscale) of ESO 184-G82. The resolutions are  $36'' \times 22''$  (top),  $15'' \times 11''$  (middle), and  $9'' \times 5''$  (bottom), with outermost ( $3\sigma$ ) contours of  $5 \times 10^{19} \text{ cm}^{-2}$ ,  $2 \times 10^{20} \text{ cm}^{-2}$ , and  $5 \times 10^{20} \text{ cm}^{-2}$ , respectively, and subsequent contours at  $N(\text{HI})$  intervals of  $\sqrt{2}$ . For reference, the solid line at the bottom right of each panel indicates a scale of 5 kpc at the distance of the galaxy. The dashed blue and solid red arrows mark the GRB location and the W-R region, respectively.

**Table 1.** Parameters of the GMRT HI data cubes

Synthesized Beam (arcs $\times$ arcs)	Channel width ( $\text{km s}^{-1}$ )	Noise in line-free channel ( $\text{mJy Bm}^{-1}$ )
$35.6 \times 21.5$	10.5, 7.0	1.5, 1.8
$24.6 \times 18.1$	7.0	1.6
$15.0 \times 10.5$	7.0	1.3
$9.1 \times 4.8$	7.0	1.0

intensity-weighted HI 21 cm velocity field of the full HI disk, displayed in contours in Fig. 3 at a low resolution ( $36'' \times 22''$ ), shows the presence of an overall gradient from the south-east to the north-west. However, even at this coarse resolution, there are multiple features incompatible with an origin in a regularly rotating disk galaxy. For a more detailed study of the velocity field, we use the data cube of resolution  $25'' \times 18''$ , which allows us to spatially distinguish different HI emission regions, while retaining some sensitivity to low  $N(\text{HI})$  gas. The HI 21 cm velocity field at this resolution is shown in greyscale in Fig. 3. The rotation of the neutral gas around the galaxy’s optical centre is evident at this resolution; the velocity field traced by H- $\alpha$  emission in a limited region around the optical centre (Christensen et al. 2008) is consistent with it.

Fig. 4 shows the HI 21 cm emission from individual ( $7 \text{ km s}^{-1}$ ) velocity channels of the  $25'' \times 18''$  data cube. A number of HI 21 cm emission regions with velocities unrelated to the main rotational gradient of the HI distribution are easily identified in the channel maps. Table 2 lists the locations of four such regions, conservatively identified in at least two velocity channels. The previously mentioned isolated knot of high- $N(\text{HI})$  gas is also identified and marked (region c). For each region, we have identified the velocity range over which the “offset” HI 21 cm emission is detected (listed in column 3 of Table 2). We use the fluxes from the “offset” regions in velocity channels where they are detected to estimate their HI masses. Column 4 of the table lists the mass fraction of each region (relative to the total HI mass of ESO 184-G2, measured at the same spatial resolution). These estimates provide a conservative lower limit to the total amount of disturbed gas in the galaxy, as they only include the mass of regions that are spatially distinct from the gas undergoing regular rotation and also only include regions identified in more than one velocity channel. Summing the mass fractions of the four kinematically disturbed regions, we find that at least 21% of the HI in ESO 184-G2 appears to not be following the rotation of the main gas disk. The largest HI region with disturbed kinematics has  $\sim 12\%$  of the total HI mass of the galaxy, and is located close to the south-eastern peak of the main body of the rotating gas. To clearly discern the presence of the large amount of disturbed HI close to the rotating disk, we show a position-velocity cut along the major axis of the galaxy in Fig. 5. This kinematically-disturbed HI is centred at an angular offset of  $-30''$  from the galaxy centre and is clearly separate from the gradient representing the main rotating gas in ESO 184-G82.

### 3 DISCUSSION AND CONCLUSIONS

The GRB host galaxy ESO 184-G82, a barred spiral galaxy, is a low-luminosity object with  $L_B = 0.05 L_B^*$ , but is clearly undergoing active star formation (Fynbo et al. 2000; Sollerman et al. 2005). The overall SFR and dust properties of the galaxy are consistent with those of local dwarf galaxies (Michalowski et al. 2009). The galaxy has an oxygen abundance of 0.41 solar (Sollerman et al. 2005; Christensen et al. 2008) and a stellar mass of  $4.8 \times 10^8 M_\odot$  (Michalowski et al. 2014). The HST image of the galaxy shows that

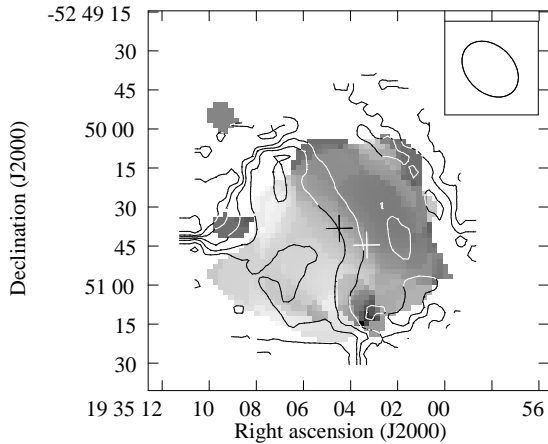


**Figure 3.** The HI 21 cm velocity field of ESO 184-G82, at two resolutions,  $36'' \times 22''$  (contours, ranging, in intervals of  $7 \text{ km s}^{-1}$ , from  $2553 \text{ km s}^{-1}$  at the bottom left to  $2609 \text{ km s}^{-1}$  at the top right) and  $25'' \times 18''$  (greyscale, from  $2550 \text{ km s}^{-1}$  as lightest to  $2630 \text{ km s}^{-1}$  as darkest). Crosses mark the locations of the galaxy’s optical centre and the GRB.

**Table 2.** Offset HI regions

Region	RA (h m s)	Dec (d'")	Channel spread ( $\text{km s}^{-1}$ )	Percentage mass
a	19 35 6.7	-52 51 04	2553.2-2602.1	12
b	19 35 2.1	-52 51 20	2560.2-2574.2	04
c†	19 35 9.4	-52 49 55	2581.2-2588.2	02
d	19 35 9.0	-52 50 31	2595.2-2602.1	03
e	19 35 3.6	-52 51 07	2623.1-2630.1	02

† Region c is spatially, not kinematically, offset from the main disk.

its optical appearance is dominated by several high surface brightness star-forming regions, especially in the southern spiral arm of the galaxy. The GRB occurred in one of these HII regions, whose properties (e.g. SFR, reddening, stellar mass) are similar to those of other HII regions in the galaxy (Christensen et al. 2008).

We find ESO 184-G82 to be a gas-rich galaxy, with an HI mass  $\sim 2.1$  times its stellar mass, which is consistent with the above studies showing ongoing star formation. Its SFR estimates, determined from H- $\alpha$  and U-V emission, lie in the range  $0.25 - 0.45 \text{ M}_{\odot} \text{ yr}^{-1}$  (Sollerman et al. 2005; Christensen et al. 2008; Michalowski et al. 2009; Castro Cerón et al. 2010). The HI mass and SFR of ESO 184-G82 are consistent with the relation between the two quantities in nearby, HI-selected galaxies (Doyle & Drinkwater 2006). Similarly, the sum of the HI and the stellar mass, and the HI 21 cm velocity width are consistent with the baryonic Tully-Fisher relation determined for nearby galaxies (Zaritsky et al. 2014). Thus, ESO 184-G82 appears to be a fairly typical star-forming galaxy, based on its global HI properties.

However, the unique feature of ESO 184-G82 is a region with a strong signature of W-R stars located at a projected distance of  $\sim 800 \text{ pc}$  from the GRB location (Hammer et al. 2006). This very young (a few Myr) star-forming region is possibly going through its first episode of star formation (Le Floch et al. 2012), with  $s\text{SFR} \sim 11.3 \text{ Gyr}^{-1}$  (using the SFR estimate from the H $\alpha$  emission; Christensen et al. 2008), which is more than an order of magnitude larger than the overall  $s\text{SFR}$  of the galaxy. This W-R region, many of whose properties are similar to those of high-redshift GRB host galaxies, is one of the most luminous and infrared-bright HII

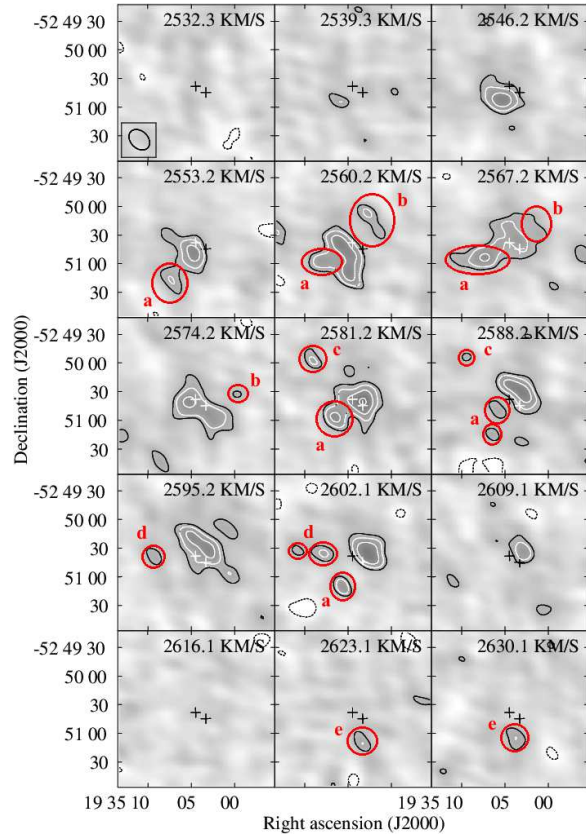


**Figure 4.** HI 21 cm emission from individual ( $7 \text{ km s}^{-1}$ ) velocity channels at  $25'' \times 18''$  resolution. Crosses mark the locations of the galaxy’s optical centre and the GRB. The outermost positive (solid) contour is at  $2.5 \sigma$  level ( $7 \times 10^{19} \text{ cm}^{-2}$ ), with each subsequent contour spaced at intervals of  $\sqrt{2}$ ; the negative (dashed) contours are at  $-2.5 \sigma$  level. Regions with offset velocity (see main text) are marked in the channels in which they appear, following the nomenclature of Table 2.

regions identified to date in the nearby Universe. It contributes substantially to the host emission at the far-infrared, millimetre, and radio wavelengths – something rarely observed in similar galaxies (Le Floch et al. 2006, 2012; Michalowski et al. 2009, 2014). The total infrared luminosity of the W-R region is  $5 \times 10^8 \text{ L}_{\odot}$ , which places it at the very bright end of the luminosity function of HII regions. Moreover, it has one of the highest star formation densities amongst isolated HII regions. Similar extra-nuclear, compact, star-forming complexes are rare, and usually found in starburst galaxies with far higher mass and SFR (Le Floch et al. 2012). We note that it has been suggested that the progenitor of the GRB was a runaway massive star ejected from this high stellar density W-R region (Hammer et al. 2006).

The origin of this W-R region has so far not been clear. Spectroscopic observations show that the six galaxies in the field of ESO 184-G82 are not associated with it, and hence, interactions with them could not have triggered such an episode of star formation (Foley et al. 2006). The HI 21 cm data, in agreement with the findings from optical spectroscopy, do not show any evidence of a large companion that might distort the velocity field of ESO 184-G82 via tidal interactions or a major merger. But interestingly, our detailed study of the spatial and kinematic structure of the HI in the galaxy shows that the gas is significantly disturbed, with more than 21% of the gas mass not following the rotation of the main gas disk.

There are several cases in the literature where galaxies with small companions (with  $\sim 10\%$  of the galaxy mass), or even no detected companions, show peculiar HI structure and/or disturbed HI kinematics; the disturbed velocity field in such systems is believed to arise from minor mergers (for e.g. see Sancisi et al. 2008). This is a likely scenario for ESO 184-G82. The encounter that led to the disturbed HI distribution must have taken place relatively recently, given that its tidal effects have not been damped out by the rotation of the galaxy and the disturbed gas has remained rotationally mis-aligned with the main disk. This puts an upper limit of a few hundred Myrs, equal to the rotation period of the galaxy disk, on the time of occurrence of the encounter. Conversely, the presence of kinematically disturbed gas regions throughout the HI disk (see Figure 4) suggest that the encounter occurred sufficiently early on for its tidal effects to disrupt the entire HI disk. Indeed, this disruption is likely to have given rise to the W-R region. This hypothesis is corroborated by the piling up of high HI column density, clumpy gas on the west side of the galaxy, which suggests shock compression of the gas, forming a high density region in which the W-R region and GRB are located, and possibly giving rise to extreme star formation. The disturbed HI kinematics and spatial structure of ESO 184-G82 hence suggests that a minor merger in the recent past is the likely cause of the uncommon properties of the W-R region in the galaxy, which, in turn, may have led to the formation of the gamma ray burst. Finally, we obtain  $N(\text{HI}) > 5 \times 10^{20} \text{ cm}^{-2}$  (higher than the damped Lyman- $\alpha$  threshold of  $2 \times 10^{20} \text{ cm}^{-2}$ ; Wolfe et al. 2005), towards the GRB location. This is consistent with the high  $N(\text{HI})$  values typically obtained in absorption studies of GRB host galaxies at  $z \gtrsim 2$  (e.g. Fynbo et al. 2009). Here, with the first HI 21 cm emission mapping of a GRB host, we show that the close environment of the GRB is coincident with the highest  $N(\text{HI})$  region of the galaxy (see Fig. 2). To confirm whether high column densities are typical of GRB environments, systematic high resolution HI 21 cm emission mapping of a sample of GRB host galaxies is required.

## ACKNOWLEDGMENTS

We thank Johan Fynbo, Jayaram Chengalur, and especially Palle Møller, for very helpful discussions and comments. We also thank the referee, Ger de Bruyn, for a detailed and helpful report. NK thanks the DST for support via a Swarnajayanti Fellowship. We thank the GMRT staff for having made possible the observations used in this paper. The GMRT is run by the National Centre for Radio Astrophysics of the Tata Institute of Fundamental Research. This paper includes archived data obtained through the Australia Telescope Online Archive. Some of the data presented in this paper were obtained from the Mikulski Archive for Space Telescopes (MAST). STScI is operated by the Association of Universities for Research in Astronomy, Inc., under NASA contract NAS5-26555. Support for MAST for non-HST data is provided by the NASA Office of Space Science via grant NNX13AC07G and by other grants and contracts.

## REFERENCES

Arabsalmani M., Møller P., Fynbo J.P.U., Christensen L., Freudling W., Savaglio S., Zafar T., 2015, MNRAS, 446, 990  
 Begum A., Chengalur J.N., Karachentsev I.D., Sharina M.E., Kaisin S.S., 2008, MNRAS, 386, 1667

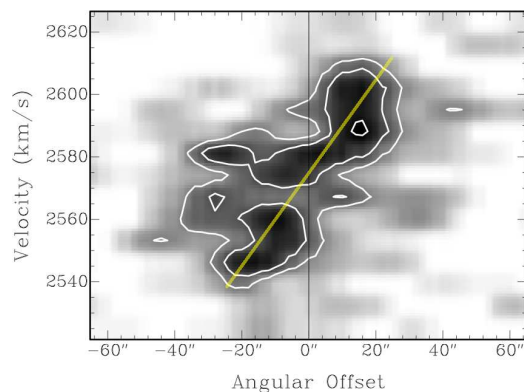


**Figure 5.** A position-velocity cut through the  $25'' \times 18''$  spectral cube along the major axis of the galaxy (PA:  $\sim 130^\circ$  east of north). The angular offset increases from south-east to north-west, with the galaxy centre at zero angular offset. The outermost contour is at the  $3\sigma$  level ( $8.4 \times 10^{19} \text{ cm}^{-2}$ ), with each subsequent contour spaced in intervals of  $\sqrt{2}$ . Fluxes are measured within a beam centred at each pixel along the p-v cut. The faint yellow line indicates the main rotating gas disk.

Bloom J.S., Kulkarni S.R., Djorgovski S.G., 2002, AJ, 123, 1111  
 Bolatto A.D., Wolfire M., Leroy A.K., 2013, ARA&A, 51, 207  
 Castro Cerón J.M. et al., 2010, ApJ, 721, 1919  
 Catinella B., Cortese L., 2015, MNRAS, 446, 3526  
 Christensen L., Vreeswijk P.M., Sollerman J., Thöne C.C., Le Floc'h E., Wiersema K., 2008, A&A, 490, 45  
 D'Elia V. et al., 2014, A&A, 564, 38  
 Doyle M. T., Drinkwater M. J., 2006, MNRAS, 372, 977  
 Foley S., Watson D., Gorosabel J., Fynbo J.P.U., Sollerman J., McGlynn S., McBreen B., Hjorth J., 2006, A&A, 447, 891  
 Fruchter A.S. et al., 2006, Nature, 441, 463  
 Fynbo J.P.U. et al., 2009, ApJSS, 185, 526  
 Fynbo J.U. et al., 2000, ApJ, 542, 89  
 Galama T.J. et al., 1998, Nature, 395, 670  
 Hammer F., Flores H., Schaerer D., Dessauges-Zavadsky M., Le Floc'h E., Puech M., 2006, A&A, 454, 103  
 Hatsukade, B., Ohta, K., Endo, A., Nakanishi, K., Tamura, Y., Hashimoto, T., Kohno, K., 2014, Nature, 510, 247  
 Krühler T. et al., 2013, A&A, 557, 18  
 Le Floc'h E. et al., 2012, ApJ, 746, 7  
 Le Floc'h E., Charmandaris V., Forrest W.J., Mirabel I.F., Armus L., Devost D., 2006, ApJ, 642, 636L  
 Massey P., Henning P. A., Kraan-Korteweg R. C., 2003, AJ, 126, 2362  
 Michalowski M.J. et al., 2014, A&A, 562, A70  
 Michalowski M.J. et al., 2009, ApJ, 693, 347  
 Prasad J., Chengalur J. N., 2012, Exp. Astron., 33, 157  
 Prochaska J.X. et al., 2009, ApJ, 691, L27  
 Prochaska J.X., Chen H., Wolfe A.M., 2008, ApJ, 672, 59  
 Sancisi R., Fraternali F., Oosterloo T., van der Hulst T., 2008, AAR, 15, 189  
 Sollerman J., Östlin G., Fynbo J.P.U., Hjorth J., Fruchter A., Pedersen K., 2005, New Astronomy, 11, 103  
 Stanway E.R., Levan A.J., Tanvir N.R., Wiersema K., van der Laan T.P.R., 2015, ApJ, 798, L7  
 Wolfe A.M., Gawiser E., Prochaska J.X., 2005, ARA&A, 43, 861  
 Zaritsky D. et al., 2014, AJ, 147, 134

This paper has been typeset from a  $\text{\TeX}/\text{\LaTeX}$  file prepared by the author.